Available online at www.sciencedirect.com
SCIENCE DIRECT
Journal of Catalysis 237 (2006) 118–130
JOURNAL OF CATALYSIS
www.elsevier.com/locate/jcat

A novel approach to synthesizing highly active Ni_2P/SiO_2 hydrotreating catalysts

Shaofeng Yang, Changhai Liang, Roel Prins *

Institute for Chemical and Bioengineering, Swiss Federal Institute of Technology (ETH), 8093 Zürich, Switzerland

Received 19 August 2005; revised 9 October 2005; accepted 10 October 2005

Available online 28 November 2005

Abstract

Silica-supported nickel phosphide particles with high dispersion were obtained by treating nickel metal particles on a support with 10% PH_3/H_2. Because the phosphidation occurred at relatively low temperature, the small nickel phosphide particles had the same size as the metal particles, and this size was maintained. The resulting catalysts were characterized by CO and O_2 chemisorption, XRD, and ^{31}P MAS NMR spectroscopy. The influence of the nickel source on the metal dispersion of the catalysts was investigated. The resulting silica-supported nickel phosphide catalysts proved to be very active in the hydrodesulfurization of dibenzothiophene and the hydrodenitrogenation of *o*-methylaniline in the presence and absence of H_2S.

Keywords: Nickel phosphide; Phosphine; Chemisorption; MAS NMR spectroscopy; Hydrodesulfurization; Hydrodenitrogenation

1. Introduction

The removal of sulfur and nitrogen atoms from oil fractions has become increasingly important as a result of the new legislation in many countries in 2005 that requires <50 ppm sulfur in gasoline and diesel. By 2010, this amount will be reduced to 10 ppm [1]. To reach these low levels of sulfur, much of the research over the past decade has aimed at improving the classic catalysts, which are based on molybdenum sulfide and promoted with cobalt or nickel [2–5], as well as at finding new catalyst materials [6–22]. Metal carbides and nitrides proved to be very active in hydrodesulfurization (HDS) and hydrodenitrogenation (HDN) but were unstable [3,9]. Under HDS conditions, they transformed into metal sulfides with normal activity. Metal phosphides have attracted recent attention not only because they are very active, but also because they are much more stable than metal carbides and nitrides with regard to hydrogen sulfide [10–24]. Although the surfaces of molybdenum and nickel phosphide take up sulfur atoms under HDS conditions, the kernel of the metal phosphide particles remains intact [23,25].

All recent studies of supported metal phosphides were performed with catalysts produced by heating a metal salt together with ammonium phosphate in hydrogen [15–24]. This simple method, which was described in the 19th century for the preparation of unsupported metal phosphides [26–28], was first used by Robinson et al. [10] to prepare a phosphorus-promoted Ni/SiO_2 catalyst and was developed further by Oyama et al. [11,13,15,18,20,21,24] for metal phosphide hydrotreating catalysts. This method has the advantage of being easy to use but has the disadvantage of requiring a high temperature for metal phosphide preparation. This leads to large catalyst particles and relatively low catalytic activity. Most other methods for preparing metal phosphides, such as the solid-state reaction of metal elements and phosphorus [29] and the electrolysis of fused salts [30], also require high temperature and/or high pressure, and obtaining small particles is difficult under such conditions. Recently the preparation of Ni_2P nanocrystallites under mild conditions was carried out using a surfactant-aided solvothermal method and the reaction between $NiCl_2 \cdot 6H_2O$ and elemental phosphorus [31,32]. Unfortunately, this method is unsuitable for the synthesis of supported metal phosphide catalysts.

* Corresponding author. Fax: +41 44 6321162.
E-mail address: roel.prins@chem.ethz.ch (R. Prins).

0021-9517/$ – see front matter
doi:10.1016/j.jcat.2005.10.021

Temperature-programmed reduction experiments of supported metal salts and phosphates have shown that even metal ions that are difficult to reduce are reduced before the phosphate ions [21,22]. The P–O bond is strong, and its reduction requires high temperature. Hydrogen atoms are available only after metal particles have formed and dissociate hydrogen molecules to hydrogen atoms. These active hydrogen atoms can spill over to the phosphate and reduce it to phosphorus or phosphine. The phosphorus or phosphine can then react with the metal particles to form metal phosphide. The strong P–O bond and the surface diffusion of the H atoms are responsible for the high reduction temperature for the phosphate. The high temperature also leads to the almost exclusive formation of phosphorus because, unlike hydrogen sulfide, phosphine is unstable at high temperature [33,34].

It seems unlikely that the phosphate reduction method can be modified so that a preparation method can be found that will give much better dispersion of the resulting metal phosphide particles. Thus we have looked for phosphorus-containing species that contain P–X bonds, which are easier to break than the P–O bond in phosphates and phosphites. In 1996, Robinson et al. reported several methods for adding phosphorus to supported Ni and studied the HDN activity of quinoline of the resulting material [10]. In one of their preparation methods they used phosphine, but only a few experiments were described. In this paper we show that by treating reduced metal particles on a support with phosphine, supported metal-phosphide particles of high dispersion can be obtained. High temperatures are unnecessary, and, consequently, the metal-phosphide particles are as small as the metal particles, and this size can be maintained. The activities of the nickel phosphide catalysts were tested in the HDN of *o*-methylaniline (OMA) and the HDS of dibenzothiophene (DBT). We recently published a preliminary report of our findings [35].

2. Experimental

2.1. Catalyst preparation

SiO_2-supported nickel phosphide catalysts were prepared by the reaction of supported Ni metal with PH_3. The supported metal precursor was prepared by pore-volume impregnation. The silica support (Merck; surface area, 500 m^2/g; 63–90 μm; pore volume after drying, 1 ml/g) was dried at 373 K for 12 h before impregnation. To investigate the influence of the nickel source on the metal dispersion of the catalysts, a solution of nickel nitrate, $Ni(NO_3)_2 \cdot 6H_2O$ (Fluka, p.a.); a solution of nickel acetate, $Ni(CH_3COO)_2 \cdot 4H_2O$ (Fluka, p.a.); and a solution containing the nickel nitrilotriacetate complex, $[Ni(NTA)]^-$ (NTA, Fluka, p.a.), were used to impregnate the silica support. The corresponding samples are referred to as N-X (nitrate), A-X (acetate), and NTA-X, respectively, where X indicates the wt% of nickel in the samples.

The $[Ni(NTA)]^-$ solution was prepared as described previously by dissolving $Ni(NO_3)_2 \cdot 6H_2O$ and NTA in an aqueous solution of ammonia (25%, Fluka, p.a.) and adjusting the pH of the solution to 7.5 with diluted NH_3 or HNO_3 [2]. Drops of these three solutions were added to the silica support until incipient wetness was achieved, followed by drying at 373 K for 12 h. The dry solid was subsequently reduced in H_2 at a flow rate of 100 ml/min in a temperature-controlled manner from room temperature (RT) to 673 K and kept at 673 K for another 2 h. For the NTA-containing precursor, the heating rate was 5 K/min. For the samples impregnated with the nickel nitrate and nickel acetate solutions, the temperature was increased from RT to 573 K at a rate of 2 K/min and then from 573 to 673 K at a rate of 1 K/min. In an additional experiment, the dried powder, impregnated with the nickel nitrate solution, was also calcined at 773 K for 3 h before reduction in H_2. The reduced samples were cooled to RT in flowing H_2.

The resulting Ni/SiO_2 samples were reacted with a 10% PH_3/H_2 mixture (MESSER, 20 ml/min). Because PH_3 is toxic and flammable, experiments should be carried out cautiously. The samples were heated from RT to the final temperature (323–523 K) at a rate of 5 K/min and maintained at this temperature for 2 h. They were then cooled to RT in flowing H_2 (50 ml/min), flushed with flowing He (50 ml/min) for 20 min, and passivated in a flow of 1 mol% O_2/He (30 ml/min). The passivated samples were handled in air.

For comparison, a sample with a molar ratio of $P/Ni = 0.8$ was prepared by the classical phosphate reduction method (sample NP-13; nickel loading, 13 wt%). Sample NP-13 was prepared by adding a certain amount of nickel nitrate solution dropwise to the calcined silica support until incipient wetness was reached, followed by drying at 373 K for 12 h. An aqueous solution of $(NH_4)_2HPO_4$ was then added to the dry sample. After drying at 373 K for 12 h and calcining in air at 773 K for 3 h, the sample was reduced in flowing hydrogen (100 ml/min) while the temperature was increased from RT to 673 K at a rate of 5 K/min and from 673 to 873 K at a rate of 2.5 K/min and then maintained at 873 K for 2 h. Then the sample was cooled to RT in flowing H_2, flushed with flowing He for 20 min, and then passivated in a 30-ml/min flow of 1 mol% O_2/He.

2.2. Catalyst characterization

XRD measurements were carried out on a Siemens D-5000 powder X-ray diffractometer (Cu-K_α radiation) with Bragg–Brentano geometry. The samples were put into a 0.3-mm-diameter capillary, which was rotated during measurement. The XRD patterns were compared with the calculated patterns obtained from the Inorganic Crystal Structure Database (ICSD) using Powdercell 2.3 software. The particle size of the supported nickel metal or nickel phosphide was calculated using the Scherrer equation, $d = 0.9\lambda/\beta\cos\theta$, where d is the mean crystal size, λ is the wavelength of the X-ray radiation, β is the full width at half maximum (in radians), and θ is the diffraction angle (in degrees).

Nitrogen adsorption isotherms were measured at 77 K using a Micromeritics Tristar 3000 instrument. Approximately 0.10 g of catalyst was placed in a quartz tube. Before the measurement, the sample was degassed under He at a flow rate of 60 ml/min at RT for 30 min and at 523 K for 2 h, then cooled to RT. The surface area was determined according to the BET method.

H_2, CO, and O_2 chemisorption analyses were performed on both reduced metal precursors and phosphides in a Micromeritics ASAP 2010 apparatus under static volumetric conditions. The passivated samples were re-reduced in situ in a H_2 flow (60 ml/min) at 623 K for 2 h before the measurements.

The morphology and particle size of the samples were studied by transmission electron microscopy (TEM) on a Philips CM30ST microscope operated at 300 kV (LaB6 cathode). The material was deposited onto a perforated carbon foil supported on a copper grid. STEM images (Z contrast) were obtained using a high-angle annular dark-field (HAADF) detector. This method can image small clusters (or even single atoms) of heavy atoms in a matrix of light atoms, because the contrast is proportional to the atomic number Z.

^{31}P nuclear magnetic resonance (NMR) spectra were obtained with an Advance 400 WB Bruker spectrometer equipped with a magic-angle spinning probe tuned to 162 MHz. An external sample of 85% phosphoric acid was used as a reference. The measurements were performed at RT. Samples were packed into a 4-mm-diameter rotor and measured with spinning at 10 kHz. The spectra were obtained by applying Fourier transformation to the free induction decay signals. The isotropic shifts of the signals were obtained by comparing spectra measured at different spinning rates. The elemental analysis was carried out with laser ablation-inductively coupled plasma mass spectrometry (LA-ICP-MS) [22].

2.3. HDN and HDS activity measurements

The HDS of dibenzothiophene (DBT) and the HDN of *o*-toluidine (orthomethylaniline, or OMA) were carried out in continuous mode in a fixed-bed reactor as described previously [22,36]. A 0.2-g sample of passivated catalyst was diluted with 8 g of SiC to achieve isothermal plug-flow conditions. The catalyst was activated in situ in H_2 (100 ml/min) at 673 K for 3 h. After activation, the pressure was increased to 3.0 MPa, and the temperature was decreased to 613 K for the hydrotreating reactions. The liquid reactant was fed into the reactor by means of a high-pressure pump. The composition of the gas-phase feed was 130 kPa *n*-octane or toluene (solvents for HDN or HDS, respectively), 17 kPa heptane (GC reference for OMA and its derivatives) or 8 kPa dodecane (GC reference for DBT and its derivatives), 1 kPa DBT or 3 kPa OMA, 0–4 kPa H_2S, and 2.8 MPa H_2. The catalyst was stabilized at 613 K and 3.0 MPa for at least 12 h before samples were taken for analysis. The HDN experiments were carried out in the absence of H_2S, in the presence of H_2S, and finally after removing H_2S from the feed. Adding dimethyldisulfide to the feed resulted in a partial pressure of 0.5–4 kPa H_2S.

3. Results

3.1. X-ray diffraction

Fig. 1 shows the XRD patterns of the oxidic precursors and reduced precursors, as well as the calculated patterns of NiO and Ni (ICSD collection codes 9866 and 44767). The XRD patterns of the calcined samples (Figs. 1b and c), obtained after impregnation with the nickel nitrate solution, were in accordance with the calculated pattern of NiO. The average crystallite size of NiO was 11 nm for the 13 wt% NiO/SiO_2 precursor and 8 nm for the 5 wt% NiO/SiO_2 precursor, according to the Scherrer equation applied to the (200) diffraction peak at 43.3°. The XRD patterns of the samples reduced in H_2 (Figs. 1d and e) exhibited peaks corresponding to Ni. Using the Scherrer equation, average crystallite sizes of 10 and 8 nm (Table 1) were calculated for the 13 wt% Ni/SiO_2 and 5 wt% Ni/SiO_2 precursors, respectively, from the full width

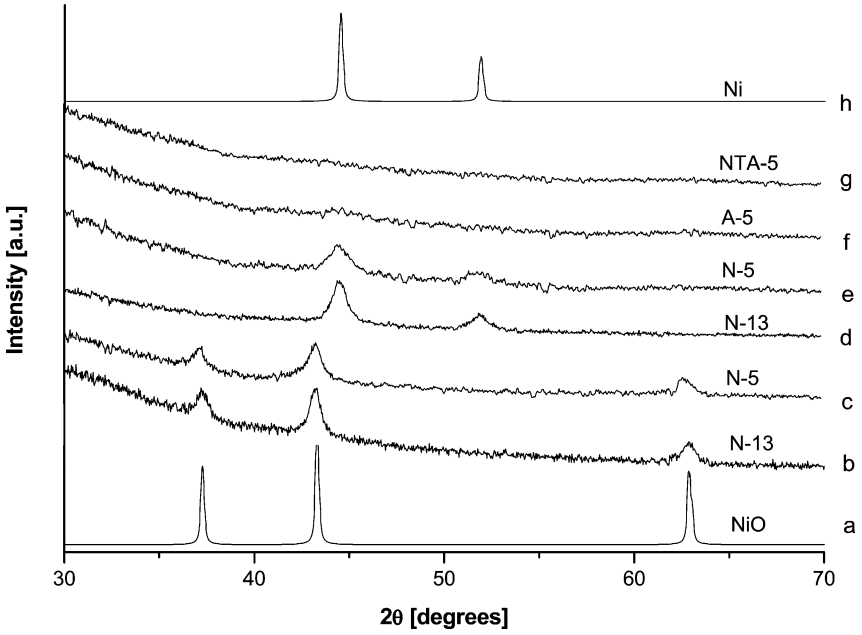

Fig. 1. XRD patterns of the calcined oxidic Ni/SiO_2 precursors (b and c), the precursors reduced in H_2 (d,e,f,g), and the calculated patterns of NiO (a) and Ni (h).

Table 1
BET, TEM, XRD and chemisorption results of the catalysts

Sample	Nickel salt precursor	Nickel loading (wt%)	BET surface area[a] (± 5 m^2/g)		Particle size (nm)							
					Ni/SiO_2				Ni_2P/SiO_2[b]			
			Ni/SiO_2	Ni_2P/SiO_2[b]	TEM	XRD	H_2[c]	O_2[c]	TEM	XRD	CO[c]	O_2[c]
NTA-5	$NH_4[Ni(NTA)]$	5	357	335	3	–	3 (149)	3 (323)	5	–	16 (51)	6 (140)
A-5	$Ni(CH_3COO)_2 \cdot 4H_2O$	5	437	381	–	–	2.4 (171)	2.3 (350)	4	–	10 (78)	4 (214)
N-5	$Ni(NO_3)_2 \cdot 6H_2O$	5	450	428	–	8	10 (40)	10 (85)	–	11	63 (13)	18 (46)
N-13	$Ni(NO_3)_2 \cdot 6H_2O$	13	439	379	10	10	13 (86)	12 (188)	15	13	90 (24)	27 (79)
NP-13	$Ni(NO_3)_2 \cdot 6H_2O$ $(NH_4)_2HPO_4$	13	–	362	–	–	–	–	–	30	46 (47)	14 (154)

[a] The surface area of the silica support is 478 m^2/g.
[b] Prepared by reaction with phosphine at 523 K, except sample NP-13.
[c] The chemisorption capacities (μmol/g_{cat}) are presented in parentheses.

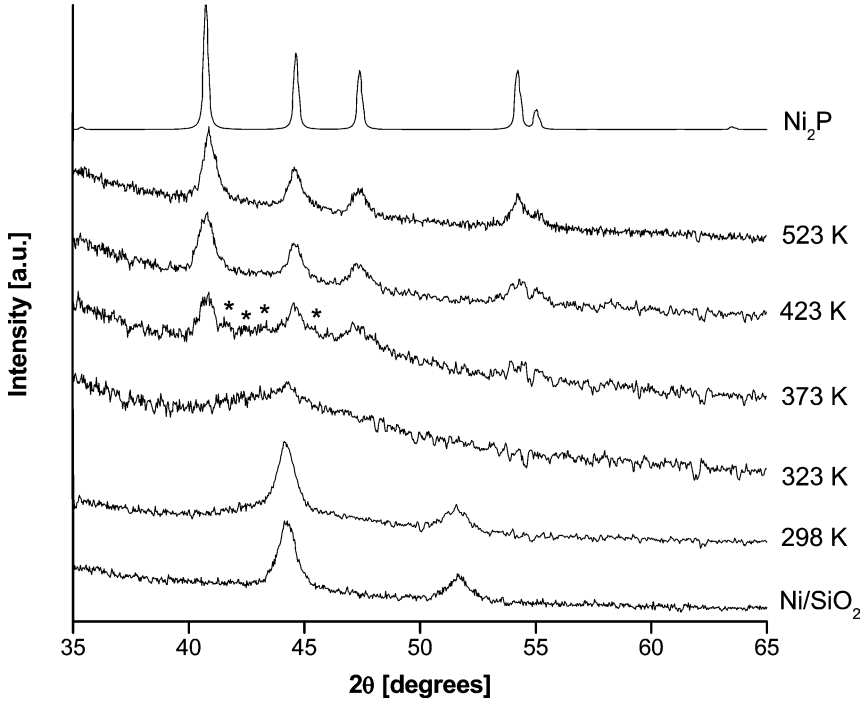

Fig. 2. XRD patterns of the 13 wt% Ni/SiO_2 samples, prepared from nickel nitrate (N-13), after reaction with phosphine at different temperatures (*, Ni_3P).

at half maximum of the (111) diffraction peak at 44.6°. In the XRD patterns of the reduced Ni/SiO_2 precursors, which were impregnated with a solution of $Ni(CH_3COO)_2 \cdot 4H_2O$ (Fig. 1f) and a solution of $NH_4[Ni(NTA)]$ (Fig. 1g), only the features of the amorphous silica were visible. This implies that the nickel particles on the silica support were too small to be detected by XRD, a finding confirmed by the TEM and hydrogen chemisorption analysis results (see below).

Fig. 2 shows the XRD patterns of the N-13 Ni/SiO_2 precursor after reaction with phosphine at different temperatures (13 wt% Ni/SiO_2, impregnated with $Ni(NO_3)_2 \cdot 6H_2O$ solution) and the calculated pattern of Ni_2P (ICSD collection code 76115). After reaction at 298 K, the diffraction characteristics of the Ni particles were still present, similar to those of the starting metallic Ni/SiO_2 precursor. The Ni peaks almost disappeared after reaction at 323 K. Only a broad peak at ca. 44.6°, belonging to Ni, remained. After reaction with phosphine at 373 K, intense peaks at 40.7°, 44.6°, and 47.4° and weaker peaks at 54.2° and 55.0°, attributed to the Ni_2P phase, appeared. Another phase was also present, indicated by very weak peaks at 41.8°, 42.8°, 43.6°, and 45.3°, all corresponding to the Ni_3P phase. When the reaction temperature was increased to 423 and 523 K, only the diffraction peaks corresponding to Ni_2P were present in the XRD patterns, indicating that Ni_2P can be achieved for the silica-supported catalyst by treating the Ni/SiO_2 precursor with phosphine at and above 423 K. The average crystallite sizes of the N-13 Ni_2P/SiO_2 catalysts, obtained at 473 and 523 K, are both ca. 13 nm, according to the Scherrer equation applied to the (111) diffraction peak at 40.7°. Further heat treatment (623 K, in flowing Ar) of the sample after reaction with phosphine at 323 K (Fig. 3b) resulted in the formation of Ni_2P (Fig. 3c).

Fig. 4 shows the XRD patterns of Ni_2P/SiO_2 catalysts prepared from different precursors. The sharp XRD peaks of the Ni_2P/SiO_2 catalyst (NP-13), prepared by the classical phos-

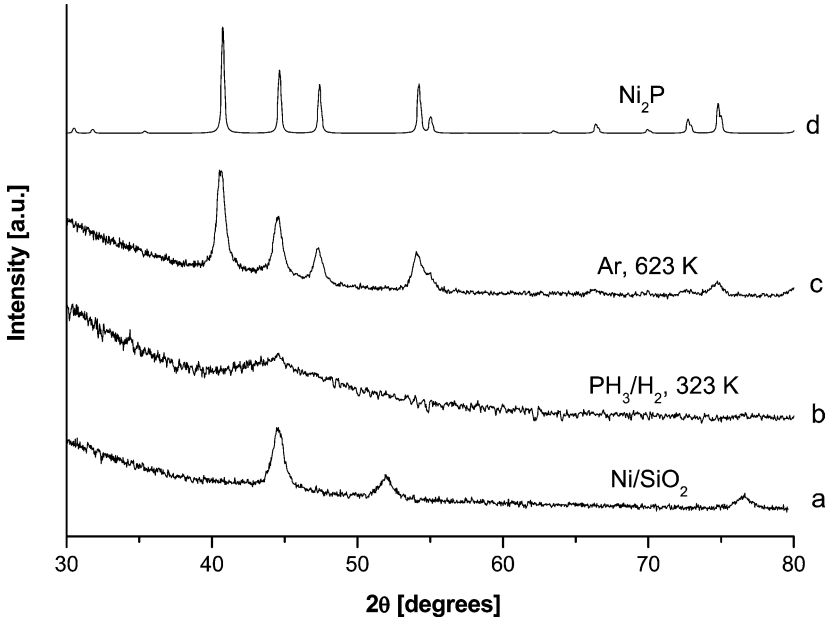

Fig. 3. XRD patterns of the 13 wt% Ni/SiO_2 precursor (a), after reaction with PH_3 at 323 K (b), and then heated in Ar at 623 K (c).

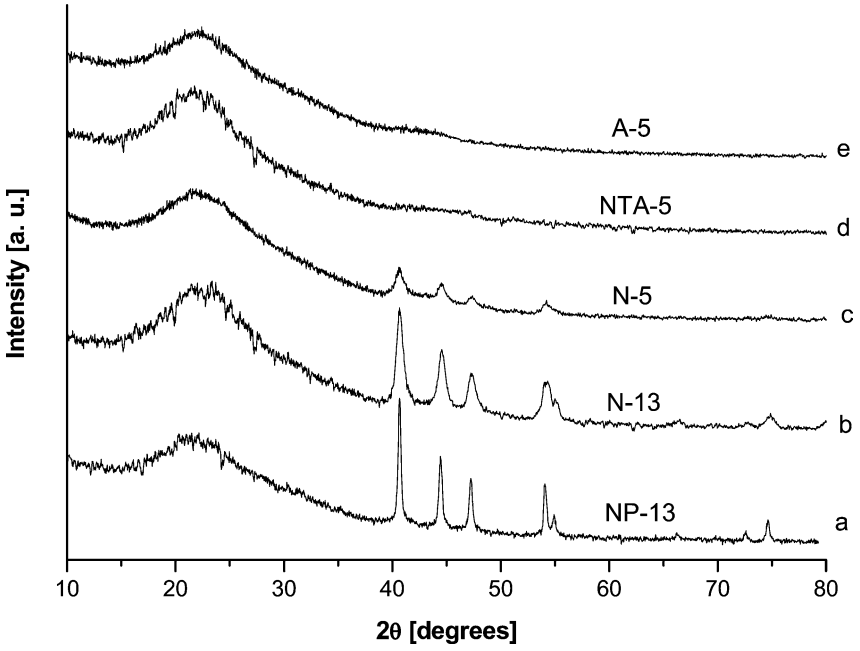

Fig. 4. XRD patterns of Ni_2P/SiO_2 catalysts prepared from different precursors.

phate reduction method, indicate the presence of large Ni_2P particles. An average crystallite size of 30 nm (Table 1) was obtained by applying the Scherrer equation to the (111) diffraction peak at 40.7°. Samples N-13 and N-5 (Figs. 4b and c) exhibited broader peaks, and average crystallite sizes of 13 and 11 nm, respectively (Table 1) were obtained. The XRD pattern of the NTA and A-5 samples show only the features of amorphous silica, implying that the nickel phosphide particles were too small to be detected by XRD.

To determine whether PH_3 also reacted with supported NiO, the calcined 13 wt% NiO/SiO_2 sample was treated with a 10% PH_3/H_2 mixture (20 ml/min) at different temperatures. After reaction with phosphine at 523 K for 2 h, the NiO XRD peaks almost disappeared, and very weak peaks at 40.7°, 44.6°, and 47.4°, attributed to the Ni_2P phase, were present (Fig. 5). When the reaction temperature was increased to 623 K, only the diffraction peaks corresponding to Ni_2P were present, indicating that silica-supported Ni_2P also can be achieved by treating the NiO/SiO_2 precursor with phosphine at or above 623 K. The average crystallite size of the resulting Ni_2P/SiO_2 catalyst is about 12 nm, according to the Scherrer equation applied to the (111) diffraction peak at 40.7°.

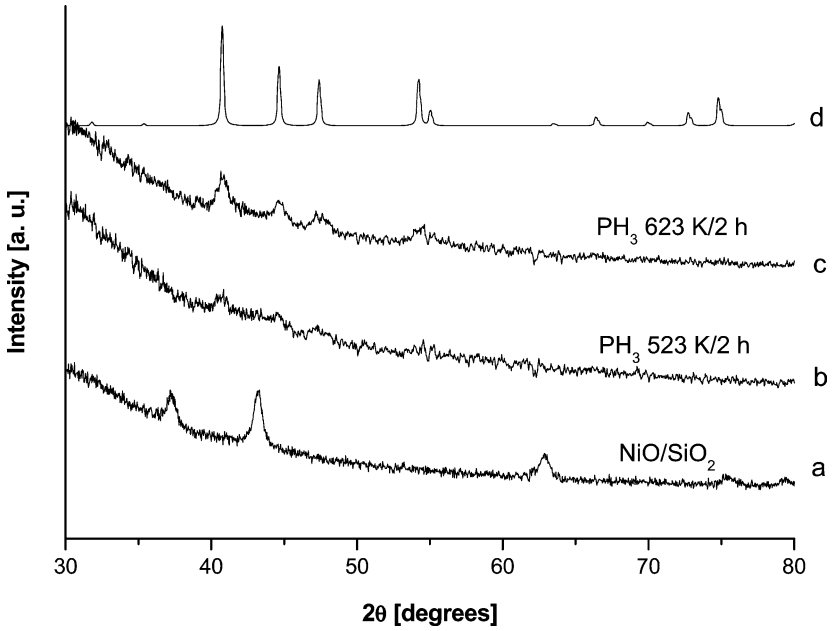

Fig. 5. XRD patterns of the calcined 13 wt% NiO/SiO_2 precursor (a), after reaction with PH_3 at 523 K (b), and 623 K (c) for 2 h.

3.2. TEM images

TEM images of sample N-13 indicate that particles formed aggregates on silica and that the size of the nickel particles ranged from approximately 5 nm to 30 nm but was mainly around 10 nm (Fig. 6a) and that the Ni_2P particles had an average diameter of ∼15 nm (Fig. 6b). These TEM results are in agreement with the XRD results (Table 1). The Ni particles in the NTA-5 sample were hardly recognizable in the high-resolution TEM images. Therefore, we performed HAADF-STEM (Z contrast) measurements, in which Ni appeared with brighter contrast than Si. Figs. 6c, d, and e reveal that the particles were better dispersed on samples NTA-5 and A-5. In sample NTA-5, the Ni particles had an average particle size of around 3 nm, and the Ni_2P particles had an average size of around 5 nm (Fig. 6d). The average size of the Ni_2P particles of sample A-5 was 4 nm (Fig. 6e). These small particle sizes agree with the absence of XRD peaks of Ni and Ni_2P for samples NTA-5 and A-5.

3.3. BET surface area and H_2, CO, and O_2 chemisorption

The BET surface areas (S_{BET}) of all of the Ni/SiO_2 and Ni_2P/SiO_2 samples were lower than those of the silica support (Table 1); the S_{BET} value of sample NTA-5 was the lowest of all. The pH of the impregnation NH_4[Ni(NTA)] solution was 7.5. At this high pH, some of the porous structure of silica may be destroyed, which may explain the relatively large loss of surface area of sample NTA-5.

H_2, CO, and O_2 chemisorption experiments were performed on both reduced metal precursors and phosphides to determine the dispersion and the active metal sites of the catalysts. Table 1 lists the H_2 and O_2 chemisorption results for the Ni/SiO_2 precursors, the CO and O_2 chemisorption results for the Ni_2P/SiO_2 catalysts, and the crystallite sizes obtained by TEM and XRD.

3.4. ^{31}P MAS NMR results

The Ni_2P structure contains two crystallographic P sites, and thus there should be two NMR signals (at 1487 and 4076 ppm) [17]. Fig. 7a shows the NMR spectra of the passivated Ni_2P/SiO_2 catalysts, synthesized at the indicated temperatures. Isotropic chemical shifts of 1487 and 4075 ppm were observed for sample NP-13, prepared by the classical phosphate reduction method. For sample N-13, prepared with PH_3 at 523 K, chemical shifts of 1478 and 4030 ppm were detected. In both samples, phosphate peaks were detected at around 0 ppm. After passivation, the spectrum of sample A-5 showed only the phosphate peaks. This may be caused by the almost complete oxidation of sample A-5, because its particle size is only about 5 nm. In agreement with this interpretation, in-situ NMR on sample A-5 showed two broad peaks at around 4058 and 1466 ppm (Fig. 7b).

3.5. Activity measurements

The hydrotreating activity of Ni_2P/SiO_2 catalysts A-5 and N-13 was tested in the HDN of OMA and HDS of DBT. For each catalyst, the HDN reactions were carried out in the absence of H_2S, in the presence of H_2S, and after removal of H_2S from the feed. The HDS reactions were carried out after the HDN reactions, without changing the catalyst.

3.5.1. HDN of OMA

The influence of H_2S on the HDN of OMA was studied at 0.5, 1, 2, and 4 kPa H_2S by adding dimethyldisulfide to the feed. The A-5 and N-13 catalysts were very active in the absence of H_2S (Figs. 8 and 9). In the presence of H_2S, the HDN activity of both Ni_2P catalysts decreased with increasing H_2S partial pressure. For the most part, the deactivation appeared to be irreversible. After H_2S was removed, the ac-

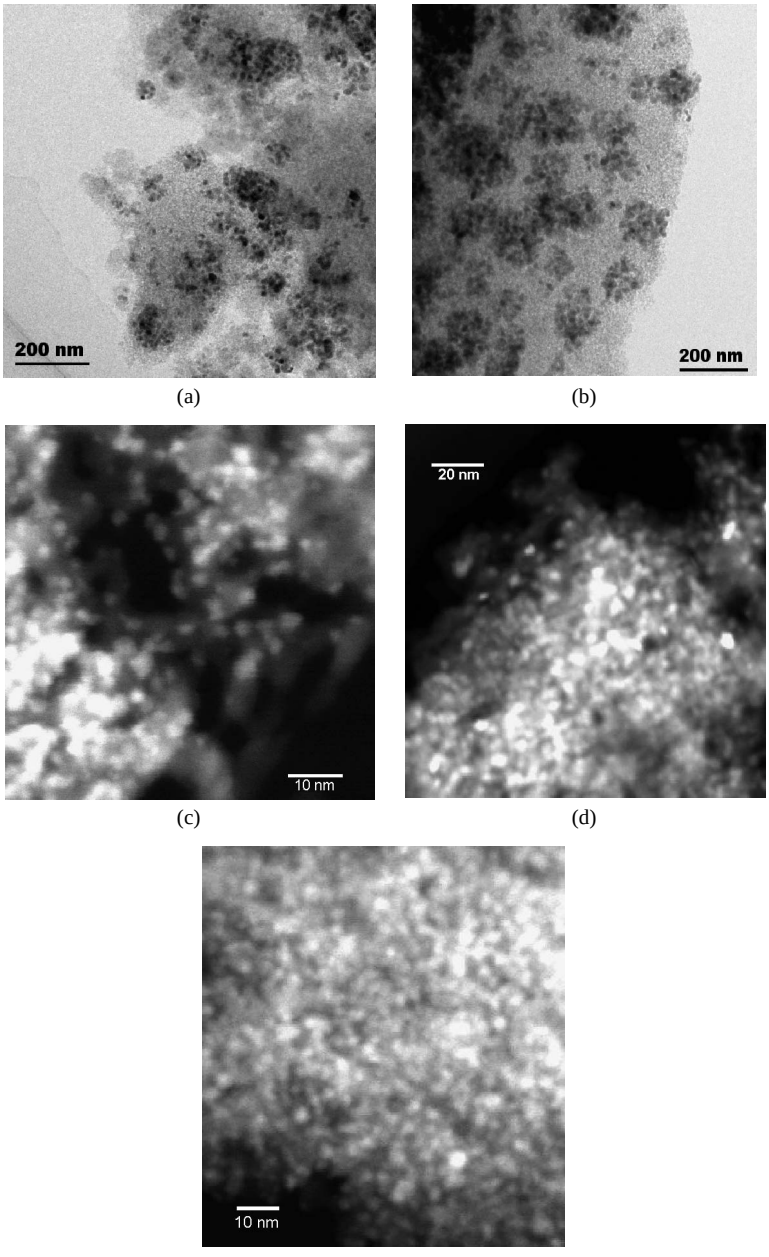

Fig. 6. TEM images of N-13 (a, Ni/SiO_2; b, Ni_2P/SiO_2) and STEM images of NTA-5 (c, Ni/SiO_2; d, Ni_2P/SiO_2) and A-5 (e, Ni_2P/SiO_2).

tivity of both catalysts increased, but not to its original level. The main reaction products of the HDN of OMA over both nickel phosphide catalysts were methylcyclohexene (MCHE), methylcyclohexane (MCH), toluene (TOL), and ethylcyclopentane (ECP). Scheme 1 presents the reaction network of the HDN of OMA over metal phosphide catalysts [22]. TOL and MCHA, the primary products, were formed through C–N bond hydrogenolysis and hydrogenation of the aromatic ring, respectively. In our experiments, MCHA was not detected. It probably reacted quickly to form MCH by direct C–N bond hydrogenolysis or by nucleophilic substitution of the amino group of MCHA by an SH group to form methylcyclohexylthiol (MCHT), followed by C–S bond hydrogenolysis. MCHT can also react quickly to MCHE, which is then hydrogenated to MCH or rearranged to ethylcyclopentene, which is hydrogenated to form ECP.

MCH was the main product over the A-5 Ni_2P/SiO_2 catalyst in the absence of H_2S, and its selectivity increased with increasing weight time. In contrast, the selectivity of MCHE decreased, indicating that this catalyst has very good hydrogenation ability. In contrast, MCHE had the highest selectivity in the presence of H_2S, and this selectivity slowly decreased with increasing weight time, indicating that H_2S strongly inhibits the hydrogenation of MCHE. The selectivities of the reaction products after the removal of H_2S were similar to those in the presence of H_2S (data not shown).

In the absence of H_2S, MCH was also the main product (at higher weight time) over the N-13 Ni_2P/SiO_2 catalyst, and its

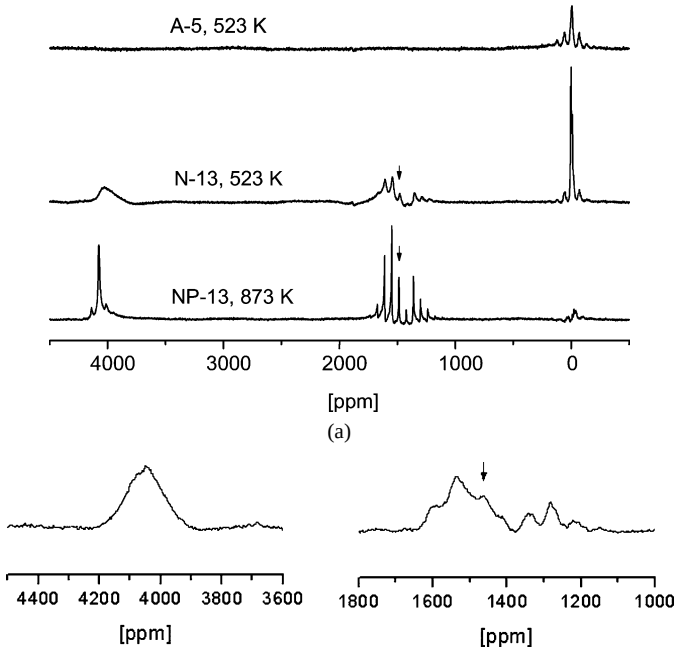

Fig. 7. (a) NMR spectra of passivated Ni_2P/SiO_2 catalysts, prepared at 523 and 873 K and (b) in situ NMR spectra of A-5 Ni_2P/SiO_2 prepared at 523 K.

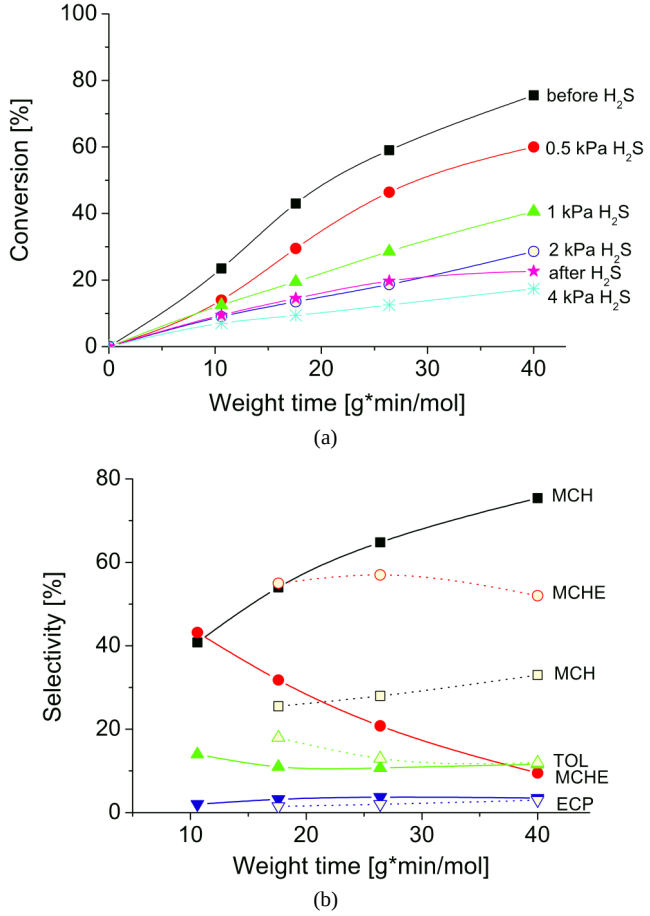

Fig. 8. HDN conversions of *o*-methylaniline before H_2S and in the presence of 0.5–4 kPa H_2S (a) and selectivities of the products (b) before H_2S (closed symbols) and in the presence of 2 kPa H_2S (open symbols) over the A-5 Ni_2P/SiO_2 catalyst.

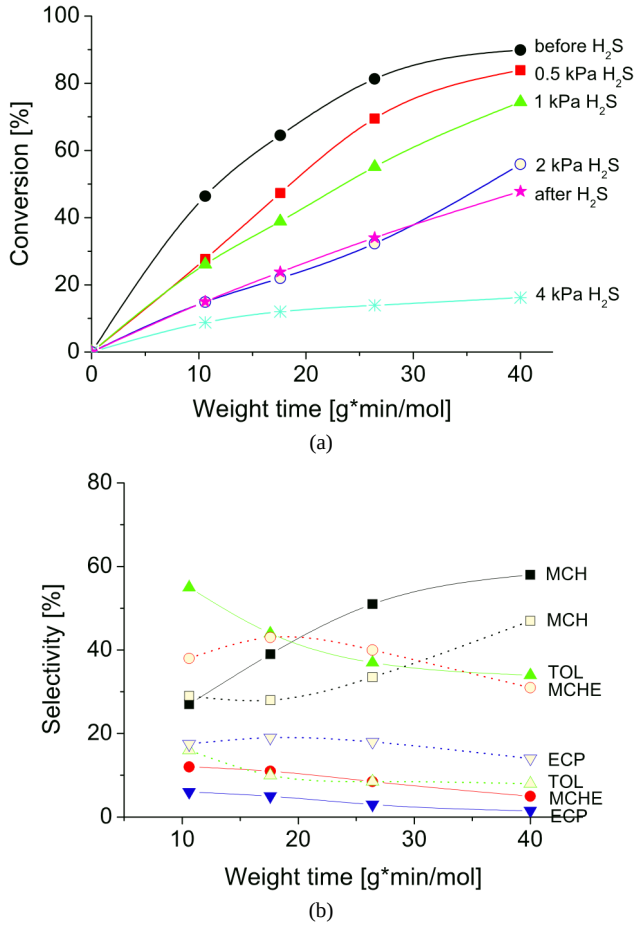

Fig. 9. HDN conversions of *o*-methylaniline before H_2S and in the presence of 0.5–4 kPa H_2S (a) and selectivities of the products (b) before H_2S (closed symbols) and in the presence of 2 kPa H_2S (open symbols) over the N-13 Ni_2P/SiO_2 catalyst.

selectivity increased with increasing weight time, similar to that over the A-5 catalyst. In contrast to the A-5 catalyst, TOL had the second-highest selectivity, which decreased with increasing weight time over the N-13 Ni_2P/SiO_2 catalyst. Over the N-13 Ni_2P/SiO_2 catalyst, the selectivity to MCH and TOL decreased in the presence of H_2S, whereas the selectivity to MCHE and ECP increased. This indicates that H_2S inhibits the C–N bond hydrogenolysis and the hydrogenation of MCHE. As for the A-5 catalyst, with the N-13 catalyst, the selectivities of the reaction products after the removal of H_2S were similar to those in the presence of H_2S (data not shown).

3.5.2. *HDS of DBT*

Three reaction products were observed in the HDS of DBT over both catalysts: biphenyl (BP), cyclohexylbenzene (CHB), and traces of tetrahydrodibenzothiophene (TH-DBT) (Figs. 10 and 11). The transformation of DBT occurs through two parallel pathways: (1) direct desulfurization (DDS), which yields BP and then BP hydrogenation yields CHB, and (2) desulfurization after hydrogenation (HYD), which first yields TH-DBT and then CHB (Scheme 2).

Over the A-5 Ni_2P/SiO_2 catalyst, the selectivity of biphenyl formation was 95% at the lowest weight time and 92% at the

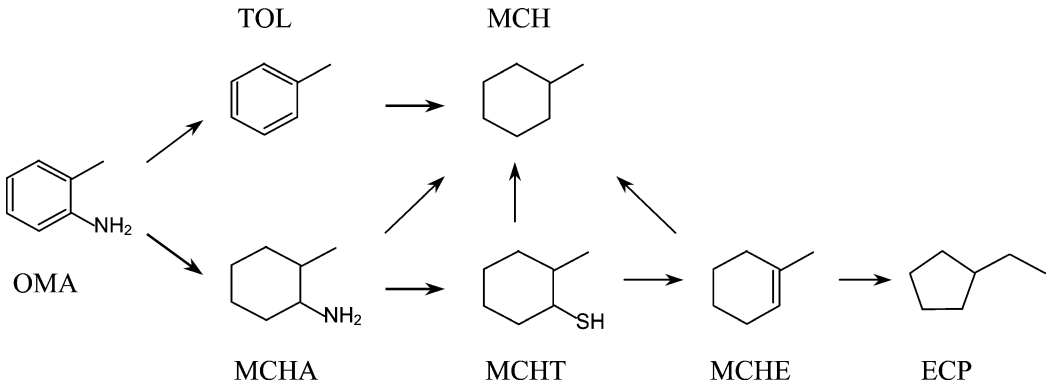

Scheme 1. Reaction network of the HDN of OMA over metal phosphide catalysts.

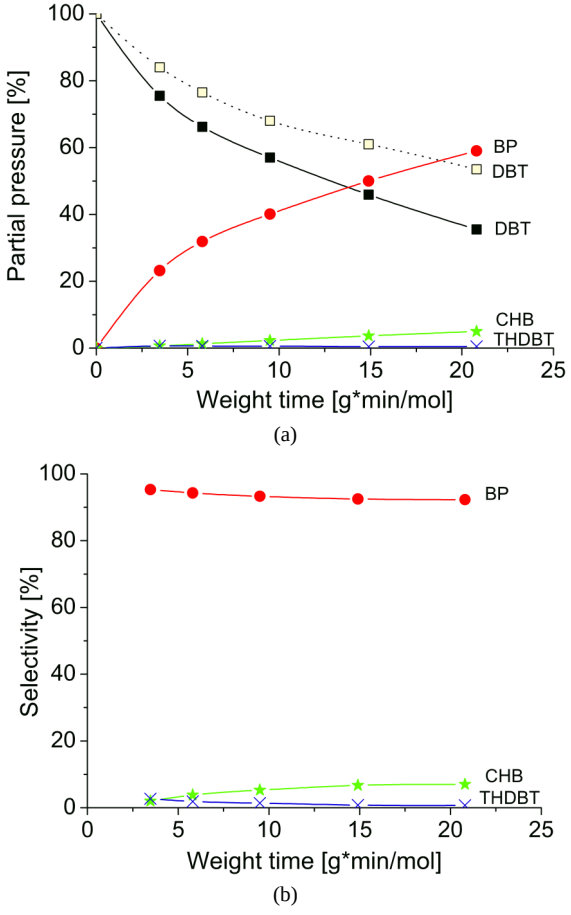

Fig. 10. Relative partial pressures (a) and selectivities of the products (b) of the HDS of DBT over the A-5 Ni_2P/SiO_2 catalyst (-□- in the presence of 1 kPa OMA).

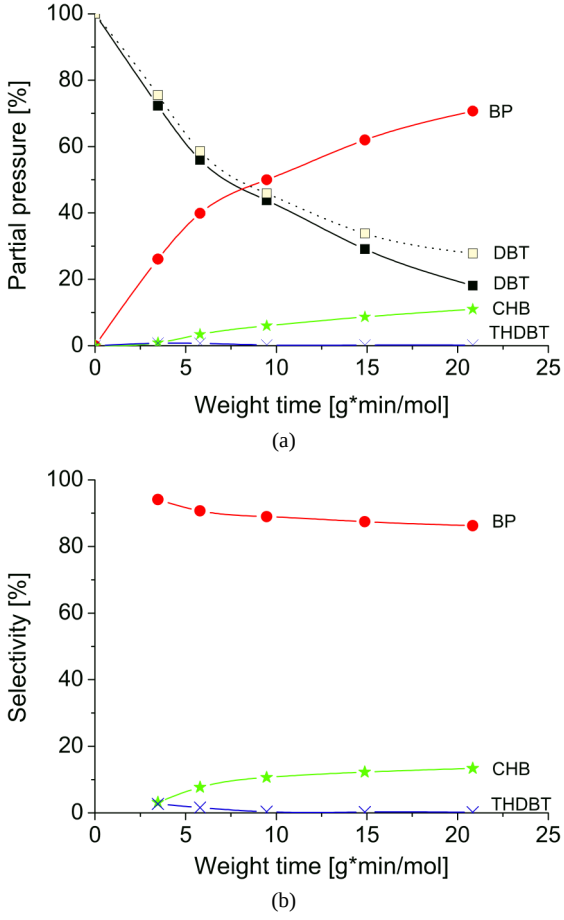

Fig. 11. Relative partial pressures (a) and selectivities of the products (b) of the HDS of DBT over the N-13 Ni_2P/SiO_2 catalyst. (-□- in the presence of 1 kPa OMA).

highest weight time (Fig. 10b). In comparison, over the N-13 Ni_2P/SiO_2 catalyst, these values were 94 and 85%, respectively (Fig. 11b). These results indicate that the DDS route was much easier than the HYD route over the Ni_2P/SiO_2 catalyst. Slow hydrogenation of biphenyl to cyclohexylbenzene occurred over both catalysts (especially over the N-13 catalyst); the biphenyl selectivity decreased with weight time, and the increase in the cyclohexylbenzene selectivity with weight time was higher than the decrease in tetrahydrodibenzothiophene selectivity.

4. Discussion

4.1. Crystallization mechanism of Ni_2P

Our results demonstrate that metal phosphide particles on a support can be easily prepared from metal or metal oxide particles by treatment with phosphine and hydrogen. The nickel particles were already fully phosphided at 423 K, whereas the NiO particles were fully phosphided at 623 K. These temperatures are much lower than the temperatures required in the phos-

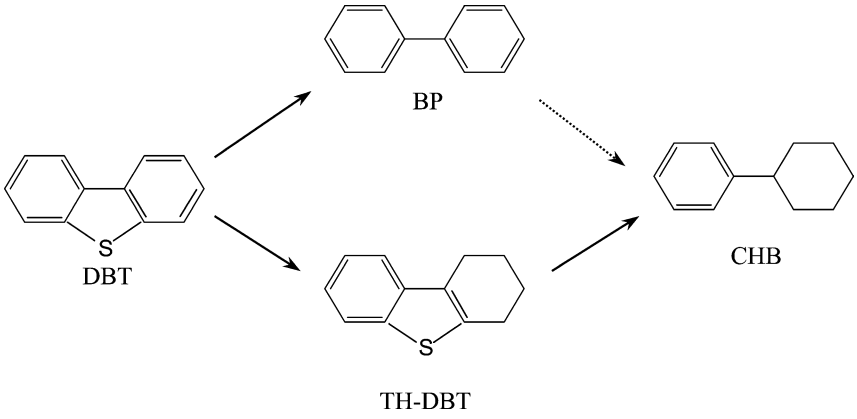

Scheme 2. Reaction network of the HDS of DBT.

phate method of preparing metal phosphide. The preparation of Ni_2P/SiO_2 catalysts according to the phosphate method [17–19] differed in the sequence of impregnation and calcination steps and in the composition (P/Ni molar ratio) of the oxidic precursors. In all of these syntheses, temperatures of ∼900–1000 K were required to achieve the formation of Ni_2P (the most active phase among the nickel phosphides) because of the very strong P–O bond. Such high temperatures lead almost exclusively to the formation of phosphorus (phosphine is unstable at high temperature), which diffuses only slowly into the metal particles, leading to sintering and loss of dispersion. It is even more difficult to synthesize supported nickel phosphides [17–19]. To obtain the desired stoichiometry, an excess of phosphorus must be added to the silica support. Thus, an Ni-to-P ratio of 2 to 1.3 was needed to synthesize Ni_2P/SiO_2 [17]. A smaller amount of phosphorus resulted in the formation of phosphides such as $Ni_{12}P_5/SiO_2$ [17–19] and Ni_3P/SiO_2 [17]. At high temperatures, phosphate also reacts with supports such as alumina; therefore, a large excess of phosphate must be added for metal phosphide particles to form on alumina [21,37]. Thus, only alumina-supported nickel phosphide catalysts with low dispersion and loading above 20 wt% have been reported [37]. The present phosphine method makes it possible to prepare highly dispersed metal phosphide particles, even on an alumina support [35]. This is important, because alumina is preferred in industry because it is thermally much more stable.

To prepare small nickel phosphide particles with the phosphine method, it is very important to prepare a precursor with a high dispersion of nickel. The most widely used method for preparing Ni/SiO_2 is impregnation with solutions of simple nickel salts, such as nickel nitrate and chloride. Alternative catalyst synthesis procedures involve homogeneous deposition precipitation, liquid-phase reduction, and impregnation of chelated precursors [38]. It was reported that the nature of the nickel precursor significantly influenced the dispersion of the supported nickel catalyst [38–40]. Usually, however, nickel nitrate is the preferred precursor in the preparation of the Ni/SiO_2 catalyst because of its high solubility in water. Nickel acetate is used less often, but a few studies have shown that well-dispersed supported Ni catalysts can be obtained with nickel acetate as the precursor [40–42]. Thermal decomposition of nickel acetate ($Ni(CH_3COO)_2 \cdot 4H_2O$) above 573 K led to a mixture of Ni^0 and NiO, which was used successfully in the catalytic decomposition of methane [42]. Using nickel acetate as a precursor thus may give Ni/SiO_2 with a higher Ni dispersion.

We have investigated the influence of the nickel source on the metal dispersion of the Ni/SiO_2 precursor by using three solutions, $Ni(NO_3)_2 \cdot 6H_2O$, $Ni(CH_3COO)_2 \cdot 4H_2O$, and $NH_4[Ni(NTA)]$ (a chelating precursor, which can complex with the surface groups of the silica support during drying [2]), to impregnate the silica support with a nickel loading of 5 wt%. XRD results showed that the highest nickel dispersion was obtained with $Ni(CH_3COO)_2 \cdot 4H_2O$ (sample A-5) and $NH_4[Ni(NTA)]$ (sample NTA-5), because no Ni diffraction peaks were detected (Fig. 1). Further characterization with H_2 and O_2 chemisorption (Table 1) showed that sample A-5 had the best nickel dispersion. We conclude, therefore, that $Ni(CH_3COO)_2 \cdot 4H_2O$ is the best of the three nickel sources for the preparation of highly dispersed Ni/SiO_2 catalysts.

The XRD results show that pure Ni_2P can be achieved on the silica-supported catalyst by treating the Ni/SiO_2 precursor with phosphine above 423 K or by treating the Ni/SiO_2 precursor with phosphine at 323 K and subsequent heating to 623 K in Ar. Similarly, Ryndin et al. [43] and Maurice et al. [44] reported that crystalline NiAs formed in the reaction of triphenylarsine ($AsPh_3$) with Ni/Al_2O_3 at 443 K. The formation of supported Ni_2P can be explained as follows. First, PH_3 decomposes on the surface of the Ni particles to form P atoms, which chemisorb on the Ni particles and form a thin NiP_x layer. At lower temperatures (e.g., 323 K), the P atoms cannot easily migrate into the metallic particles and will remain on the outer surface of the particles. Above 423 K, the P atoms migrate into the metallic particles and form first an extended amorphous Ni_xP_y phase and then a crystalline Ni_2P phase. When the sample is heated to 623 K, migration of the P atoms as well as crystallization occur, resulting in the formation of crystalline Ni_2P (Fig. 5c). The incorporation of phosphorus into the Ni particles produces an increase in the particle size from 10 nm for Ni to 13 nm for Ni_2P as shown by XRD. Considering that the lattice volumes of Ni and Ni_2P are 43.55 and 100.54 A^3, respectively, and that there are four Ni atoms and three Ni_2P units per unit cell, the diameter of a Ni_2P particle must be 1.15 times larger than the diameter of the Ni particle for the same number of nickel atoms. This value is close to the observed value.

4.2. Chemisorption

There is good agreement between the H_2 and O_2 chemisorption capacities of the four metallic Ni/SiO_2 precursors (Table 1). Assuming that the metal particles have a spherical geometry, the particle size can be estimated from the equation $d = 101/D$, where d represents the particle size in nm and D represents the metal dispersion in % [45]. Using this equation and the metal dispersion calculated from the chemisorption capacities by assuming a stoichiometry of one H atom per surface metal atom and one O_2 molecule per surface metal atom [45], the Ni particle sizes were calculated (Table 1). These values agree well with the particle sizes obtained from XRD and TEM. The agreement among these techniques for Ni/SiO_2 is comparable to that reported by Smith et al. [45].

The Ni_2P/SiO_2 catalysts were characterized by CO and O_2 chemisorption. Assuming cubic or spherical geometry, it is possible to calculate a theoretical particle size (d_t) from the chemisorption result from the equation $d_t = 6nf/\rho L$ [18], where f is the fractional weight loading of the sample, n is the average surface metal atom density (which for Ni_2P is 1.01×10^{15} atoms cm^{-2} [18]), and L is the metal site concentration obtained from CO or O_2 chemisorption by assuming one CO or O_2 molecule per surface metal atom. The crystallite sizes of the Ni_2P/SiO_2 catalysts, calculated from the CO chemisorption results, are much higher than those obtained from the TEM and XRD results (Table 1), whereas the crystallite sizes calculated from the O_2 chemisorption results (with the exception of sample NP-13) agree reasonably well with those obtained from the TEM and XRD results. Nevertheless, for all of the Ni_2P/SiO_2 catalysts, CO chemisorptions ($\mu mol/g_{cat}$) correlate well with the O_2 chemisorptions, which are greater by about a factor of three. This suggests that CO adsorbs on special nickel atoms only and O_2 adsorbs on any surface atom.

CO and O_2 chemisorption have been used before to determine the site densities of metal sulfide and phosphide catalysts. Sawhill et al. found that the HDS activities of their Ni_2P/SiO_2 catalysts correlated well with O_2 chemisorption [19]. However, several reports indicate that CO or O_2 chemisorption cannot be used to compare the HDS activity of different metal phosphides [20,46,47]. Koranyi found that the amount of chemisorbed oxygen correlates with the surface area of sulfide but not with that of phosphide in sulfided silica-supported nickel phosphide catalysts [48]. Layman and Bussell suggested that CO should be used cautiously for measuring the site densities on Ni_2P/SiO_2 catalysts [25]. In addition, the mechanisms for the chemisorption of CO and O_2 molecules on metal phosphides remain unclear. All of these results demonstrate the need to exercise care when correlating the chemisorption results with the catalytic activities of metal phosphide catalysts. Our N-13 Ni_2P/SiO_2 catalyst had higher HDS and HDN activities than the A-5 Ni_2P/SiO_2 catalyst, although its CO and O_2 chemisorption capacities were about three times lower. We suggest that CO and O_2 chemisorption cannot be used to compare the hydrotreating activity of metal phosphide catalysts prepared differently or of catalysts with significantly different particle sizes.

4.3. Hydrotreating behavior

The catalytic results demonstrate that the hydrotreating behavior of the A-5 and N-13 Ni_2P/SiO_2 catalyst differ, especially in the HDN of OMA. In the absence of H_2S, the A-5 Ni_2P/SiO_2 catalyst performs well in hydrogenation, and the N-13 Ni_2P/SiO_2 catalyst performs well both in hydrogenation and hydrogenolysis. In the absence of H_2S, the selectivity of the reaction products over the A-5 catalyst (MCH > MCHE > TOL > ECP) are similar to the selectivity obtained in the HDN of *o*-propylaniline (OPA) over unsupported Ni_2P and MoP catalysts [14]. The order of selectivity over unsupported Ni_2P was propylcyclohexane (PCH) > propylcyclohexene (PCHE) > propylbenzene (PB) when the conversion of OPA was >20%. Over the N-13 catalyst, TOL had the second-highest selectivity, similar to the selectivity over the supported MoP/SiO_2 and $NiMoP/SiO_2$ catalysts [22]. Over the MoP/SiO_2 and $NiMoP/SiO_2$ catalysts, however, the selectivity was MCHE > TOL > MCH, with MCHE as the main product.

DBT is mainly desulfurized by the DDS route over both catalysts, as over sulfided $CoMo/Al_2O_3$ and $NiMo/Al_2O_3$ catalysts [49]. The selectivity of biphenyl over the A-5 Ni_2P/SiO_2 catalyst (95% at the lowest weight time and 92% at the highest weight time) is higher than over the N-13 Ni_2P/SiO_2 catalyst (94% at the lowest weight time and 85% at the highest weight time) and much higher than over sulfided catalysts (70–80%) [49]. This may be due to the small particle size of the A-5 Ni_2P/SiO_2 catalyst. Small particles will have more edge and kink sites, on which σ adsorption of DBT molecules and direct desulfurization can occur. We also performed the HDS of DBT over $CoMo/\gamma\text{-}Al_2O_3$ and N-13 Ni_2P/SiO_2 catalyst at 573 K and a total pressure of 5 MPa. Their HDS activity is comparable; at a weight time of 5 (g min)/mol, the conversion of DBT is 32% over $CoMo/\gamma\text{-}Al_2O_3$ catalyst and 42% over N-13 Ni_2P/SiO_2 catalyst.

The N-13 Ni_2P/SiO_2 catalyst had a higher hydrotreating activity than the A-5 Ni_2P/SiO_2 catalyst. To avoid full oxidation of a fresh catalyst, the Ni_2P/SiO_2 catalysts were passivated and re-reduced in situ in H_2 at 673 K before the activity measurements to remove the passivation layer. Passivation may have an influence on the catalytic performance of the phosphide catalysts. Several studies have shown that Ni or Mo phosphides, prepared by the traditional reduction–passivation–re-reduction method, exhibit an increase in HDS activity in the first few hours of time on stream. However, this increase was not observed by Wang et al. [50] for the supported nickel phosphides prepared by in situ reduction in the hydrotreating reactor. The in situ reduction gave much better activity than the traditional reduction–passivation-re-reduction method. Therefore, Wang et al. supposed that a small amount of the nickel phosphide might be oxidized during passivation [50]. When passivated phosphides are tested in HDS reactions in flowing H_2, their phosphide structure may reform, resulting in increased HDS activity. The occurrence of passivation might be subject to experimental uncertainties. Sawhill et al. [37] recently reported that the thickness of the passivation layer on the Ni_2P particles in a 25 wt%

Ni_2P/SiO_2 catalyst is about 2 nm. In the present study, the A-5 and N-13 Ni_2P/SiO_2 catalysts had different Ni_2P particle sizes. The XRD, TEM, and chemisorption results showed that the Ni_2P particles of the A-5 catalyst are highly dispersed and consequently have a very small particle size (<5 nm), whereas the particles in the N-13 catalyst are larger (∼13 nm). Thus the Ni_2P particles of the A-5 catalyst may be almost fully oxidized during passivation, which is confirmed by the NMR spectrum in Fig. 7a. When this passivated catalyst is re-reduced in H_2 before and during the hydrotreating measurements, the Ni_2P structure may not reform completely. This may explain why the hydrotreating activity of the A-5 catalyst, which has a higher Ni_2P dispersion, is lower than that of the N-13 catalyst.

The structure of the passivation layer is still unknown. Fig. 7a shows phosphate peaks in the region around 0 ppm for all of the passivated Ni_2P/SiO_2 catalysts. Previous ^{31}P MAS NMR results of MoP/SiO_2 indicated that surface phosphate species form on passivation of a fresh MoP/SiO_2 sample and can be removed by H_2 reduction at 673 K [22]. A recent IR study of passivated MoP/SiO_2 showed that a band at 3365 cm^{-1}, attributed to the P–OH vibration of phosphate species on the surface of passivated MoP/SiO_2, disappeared on reduction in H_2 at 923 K [23]. In the present study, H_2 chemisorption measurements were also carried out on all of the passivated Ni_2P/SiO_2 catalysts after re-reduction in H_2 flow at 673 K for 2 h. However, the H_2 chemisorption capacity of all of the samples was close to zero after re-reduction, although the samples had nonzero CO and high O_2 chemisorption capacities. This suggests that the passivation layer consists not of nickel phosphate, but of Ni–P–O.

Elemental analysis of the Ni_2P/SiO_2 catalysts showed that the N-13 sample contained 12.8 wt% Ni and 4.5% wt% P (Ni/P = 1/0.67) and the A-5 sample contained 4.8 wt% Ni and 3.6 wt% P (Ni/P = 1/1.43). This indicates an excess of P on the catalysts. Similar to Oyama et al. [18], we suggest that part of the excess P resides on the surface of the Ni_2P crystallites and blocks the active sites. This could be another reason why the activity of sample A-5 is lower than that of sample N-13.

The present work demonstrates that H_2S has a strong negative effect on the HDN activity of the Ni_2P catalyst. The inhibitory effect of H_2S on the HDN of OMA and of OPA over phosphide catalysts was also observed in previous studies of unsupported Ni_2P, MoP, NiMoP, and CoMoP and of silica-supported MoP, CoP, WP, NiMoP, and CoMoP [14,22]. However, XRD measurements of the samples did not reveal any differences before or after the HDN reaction. By elemental analysis and EXAFS measurements, Oyama et al. found the formation of Ni–S linkages at the surface of the silica-supported Ni_2P particles that had been tested under HDS conditions [18]. They also observed that the position of the XRD peaks of the spent samples did not change, demonstrating that the bulk of the Ni_2P particles were stable under the hydrotreating conditions. Wu et al. [23] and Layman and Bussell [25] investigated the surface of silica-supported nickel and molybdenum phosphide catalysts by infrared spectroscopy with CO as a probe molecule. Their results showed that the surface of these phosphides can be partially sulfided and that a phosphosulfide phase forms on the surface of the catalyst in H_2S. This suggests that the active phase of the Ni_2P/SiO_2 catalyst in the HDS reaction is probably a NiP_xS_y phase in the outer region of the Ni_2P crystallites.

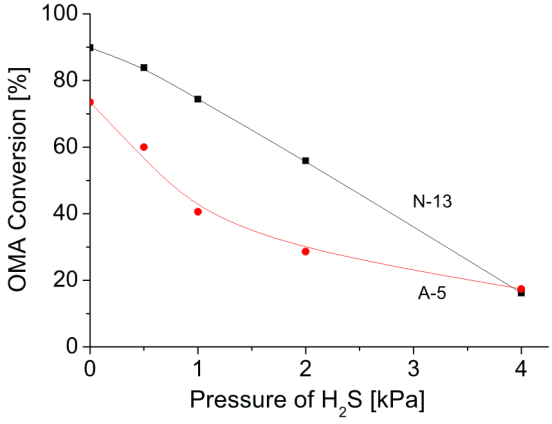

Fig. 12. Influence of H_2S on the conversion of OMA over the A-5 and N-13 Ni_2P/SiO_2 catalysts at $\tau = 40$ (g min)/mol.

H_2S has a stronger effect on the HDN activity of the A-5 catalyst than on the N-13 catalyst (Fig. 12). In the presence of 1 kPa H_2S, the conversion of OMA is 74% over the N-13 catalyst but only 40% over the A-5 catalyst, indicating that the A-5 catalyst, which has a smaller Ni_2P particle size, is more sensitive to H_2S than the N-13 catalyst. This is understandable, because the smaller the particles, the more Ni_2P present on the surface of the particle and exposed to H_2S. As discussed earlier, the surface of the Ni_2P particles can be partially sulfided in H_2S. Therefore, Ni_2P particles with smaller particle sizes can be changed more easily.

5. Conclusions

Our results demonstrate that metal phosphide particles on a support can be easily prepared from metal or metal oxide particles by treatment with phosphine and hydrogen. The phosphine method enables preparation of metal phosphide particles at moderate temperature. As a result, the particle size is equivalent to that of the precursor particle size, and supported metal phosphide particles with high dispersion can be achieved. The nickel particles became fully phosphided at 423 K, whereas the NiO particles were fully phosphided only at 623 K. $Ni(CH_3COO)_2 \cdot 4H_2O$ was the best nickel source for the preparation of highly dispersed Ni/SiO_2 and subsequent Ni_2P/SiO_2 catalysts. The resulting silica-supported nickel phosphide proved to be very active in the hydrodesulfurization of dibenzothiophene and the hydrodenitrogenation of *o*-methylaniline in the presence and absence of H_2S.

References

[1] I.V. Babich, J.A. Moulijn, Fuel 82 (2003) 607.
[2] L. Medici, R. Prins, J. Catal. 163 (1996) 28.
[3] R. Prins, Adv. Catal. 46 (2001) 399.
[4] M. Sun, D. Nicosia, R. Prins, Catal. Today 86 (2003) 173.

[5] S.K. Bej, S.K. Maity, U.T. Turaga, Energy Fuels 18 (2004) 1227.
[6] S. Ramanathan, S.T. Oyama, J. Phys. Chem. 99 (1995) 16365.
[7] J.A.R. van Veen, J.K. Minderhoud, J.G. Buglass, P.W. Lednor, L.T. Thompson, Mater. Res. Soc. Symp. Proc. 368 (1995) 51.
[8] S. Ramanathan, C.C. Yu, S.T. Oyama, J. Catal. 173 (1998) 10.
[9] S. Li, J. Lee, J. Catal. 178 (1998) 119.
[10] W.R.A.M. Robinson, J.N.M. van Gestel, T.I. Koranyi, S. Eijsbouts, A.M. van der Kraan, J.A.R. van Veen, V.H.J. de Beer, J. Catal. 161 (1996) 539.
[11] W. Li, B. Dhandapani, S.T. Oyama, Chem. Lett. (1998) 207.
[12] C. Stinner, R. Prins, Th. Weber, J. Catal. 191 (2000) 438.
[13] P. Clark, W. Li, S.T. Oyama, J. Catal. 200 (2001) 140.
[14] C. Stinner, R. Prins, Th. Weber, J. Catal. 202 (2001) 187.
[15] P. Clark, X. Wang, S.T. Oyama, J. Catal. 207 (2002) 256.
[16] D.C. Phillips, S.J. Sawhill, R. Self, M.E. Bussell, J. Catal. 207 (2002) 266.
[17] C. Stinner, Z. Tang, M. Haouas, Th. Weber, R. Prins, J. Catal. 208 (2002) 456.
[18] S.T. Oyama, X. Wang, Y.K. Lee, K. Bando, F.G. Requejo, J. Catal. 210 (2002) 207.
[19] S.J. Sawhill, D.C. Phillips, M.E. Bussell, J. Catal. 215 (2003) 208.
[20] S.T. Oyama, J. Catal. 216 (2003) 343.
[21] P.A. Clark, S.T. Oyama, J. Catal. 218 (2003) 78.
[22] V. Zuzaniuk, R. Prins, J. Catal. 219 (2003) 85.
[23] Z. Wu, F. Sun, W. Wu, Z. Feng, C. Liang, Z. Wei, C. Li, J. Catal. 222 (2004) 41.
[24] Y. Shu, S.T. Oyama, Chem. Commun. (2005) 1143.
[25] K.A. Layman, M.E. Bussell, J. Phys. Chem. B 108 (2004) 10930.
[26] H. Rose, Ann. Phys. 24 (1832) 295.
[27] H. Struve, Jahresber. Fortsch. Chem. Verw. Theile Anderer Wiss. (1860) 76.
[28] J.C. Hutter, Ann. Chim. 8 (1953) 450.
[29] A.R. West, Solid State Chemistry and Its Applications, Wiley, Chichester, 1992.
[30] M. Chene, Ann. Chim. 15 (1941) 187.
[31] J. Liu, X. Chen, M. Shao, C. An, W. Yu, Y. Qian, J. Crystal Growth 252 (2003) 297.
[32] H. Su, Y. Xie, B. Li, X. Liu, Y. Qian, Solid State Ionics 122 (1999) 157.
[33] C.E. Myers, T.J. Conti, J. Electrochem. Soc. 132 (1985) 454.
[34] A.S. Jordan, J. Vac. Sci. Technol. A 12 (1994) 204.
[35] S. Yang, R. Prins, Chem. Commun. (2005) 4178.
[36] M. Egorova, R. Prins, J. Catal. 221 (2004) 11.
[37] S.J. Sawhill, K.A. Layman, D.R. Van Wyk, M.H. Engelhard, C. Wang, M.E. Bussell, J. Catal. 231 (2005) 300.
[38] D.J. Lensveld, J.G. Mesu, A.J. van Dillen, K.P. de Jong, Microporous Mesoporous Mater. 44–45 (2001) 401.
[39] J. Chen, R. Wang, Y. Li, J. Zhang, Ranliao Huaxue Xuebao 29 (2001) 494.
[40] B. Li, R. Watanabe, K. Maruyama, K. Kunimori, K. Tomishige, Catal. Today 104 (2005) 7.
[41] A. Boudjahem, S. Monteverdi, M. Mercy, M.M. Bettahar, Appl. Catal. A 250 (2003) 49.
[42] R.A. Couttenye, M.H. De Vila, S.L. Suib, J. Catal. 233 (2005) 317.
[43] Y.A. Ryndin, J.P. Candy, B. Didillon, L. Savary, J.M. Basset, J. Catal. 198 (2001) 103.
[44] V. Maurice, Y.A. Ryndin, G. Bergeret, L. Savary, J.P. Candy, J.M. Basset, J. Catal. 204 (2001) 192.
[45] J.S. Smith, P.A. Thrower, M.A. Vannice, J. Catal. 68 (1981) 270.
[46] F. Sun, W. Wu, Z. Wu, J. Guo, Z. Wei, Y. Yang, Z. Jiang, F. Tian, C. Li, J. Catal. 228 (2004) 298.
[47] J.A. Rodriguez, J.Y. Kim, J.C. Hanson, S.J. Sawhill, M.E. Bussell, J. Phys. Chem. B 107 (2003) 6276.
[48] T.I. Koranyi, Appl. Catal. A 239 (2003) 253.
[49] M. Egorova, R. Prins, J. Catal. 225 (2004) 417.
[50] A. Wang, L. Ruan, Y. Teng, X. Li, M. Lu, J. Ren, Y. Wang, J. Catal. 229 (2005) 314.